ARTICLES SCIENCE CHINA Materials

mater.scichina.com link.springer.com

Published online 6 March 2018 | https://doi.org/10.1007/s40843-017-9221-4
Sci China Mater 2018, 61(8): 1112–1122

Rotating magnetic field-controlled fabrication of magnetic hydrogel with spatially disk-like microstructures

Fengguo Fan[1,2], Jianfei Sun[1*], Bo Chen[1], Yang Li[1], Ke Hu[3], Peng Wang[4], Ming Ma[1] and Ning Gu[1*]

ABSTRACT **Composite biomaterials with controllable microstructures play an increasingly important role in tissue engineering and regenerative medicine. Here, we report a magnetic hydrogel composite with disk-like microstructure fabricated by assembly of iron oxide nanoparticles during the gelation process in the presence of rotating magnetic field. It should be mentioned that the iron oxide nanoparticles here were synthesized identically following techniques of Ferumoxytol that is the only inorganic nanodrug approved by FDA for clinical applications. The microstructure of nanoparticles inside the hydrogel was ordered three-dimensionally due to the twist of the aligned chains of magnetic nanoparticles which leads to the lowest state of systematic energy. The size of microstructure can be tuned from several micrometers to tens of micrometers by changing the assembly parameters. With the increase of microstructure size, the magnetothermal anisotropy was also augmented. This result confirmed that the assembly-induced anisotropy can occur even for the several micron aggregates of nanoparticles. The rotating magnetic field-assisted technique is cost-effective, simple and flexible for the fabrication of composite hydrogel with ordered microstructure. We believe it will be favorable for the quick, green and intelligent fabrication of some composite materials.**

Keywords: magnetic nanoparticles, assembly, rotating magnetic field, hydrogel, intelligent fabrication

INTRODUCTION

Currently, the functional nanoparticles are increasingly involved in construction of composite biomaterials to reinforce performance in diverse aspects [1–4]. The microstructures of nanoparticles play an essential role in control of collective properties for the composite biomaterials. For instance, the artificial materials composed of nanoparticles with multi-hierarchical order have been exhibited to be more capable of mimicking the natural matters, such as artificial muscle [5], bone [6–8], spider silk [9,10] and even niche of stem cells [11,12]. Owing to its special magnetic property and clinic approval by the Food and Drug Administration (FDA), iron oxide nanoparticles are the extremely promising elemental units for the clinician. Thus, it remains critical and imperative to develop a controllable method for production of composite materials integrated with iron oxide nanoparticles. Fortunately, the magnetic nanoparticles have a significant advantage of remote manipulation with magnetic field so that the magnetic field-directed assembly of magnetic nanoparticles can be employed to form the ordered structures effectively [13–15]. For instance, the modulated magnetostatic magnetic field can direct the long-ranged order of magnetic nanoparticles in macroscopic dimension [16–18]. Furthermore, the common biomaterials have demonstrated exceptional magneto-controllable performance by integration with the magnetic nanoparticles [19–21]. It was reported very recently that the composite hydrogel internally with the chain-like assemblies of magnetic nanospheres showed the orientation-dependent magnetothermal property which can bring about the so-called electromagnetically controlled

[1] State Key Laboratory of Bioelectronics, Jiangsu Laboratory for Biomaterials and Devices, Department of Biological Science and Medical Engineering, Southeast University, Nanjing 210009, China
[2] Department of Physics, Shangqiu Normal University, Shangqiu 476000, China
[3] Key Laboratory of Clinical and Medical Engineering, Department of Biomedical Engineering, Nanjing Medical University, Nanjing 210029, China
[4] Department of Sports Medicine and Adult Reconstructive Surgery, Drum Tower Hospital affiliated to Medical School of Nanjing University, Nanjing 210008, China
* Corresponding authors (emails: sunzaghi@seu.edu.cn (Sun J); guning@seu.edu.cn (Gu N))

"on demand" release of drugs [22,23]. Mechanism of this phenomenon rooted in the assembly-dependent enhancement of energy absorption which made the Poynting's theorem take effect upon the assemblies of nanoparticles [24,25]. Thus, the larger projected area of assemblies in the direction of Poynting's vector will cause more absorption of electromagnetic energy and more thermogenesis. However, there remain at least two aspects to further explore for purpose of clinical application. For one thing, the magnetic nanospheres are incapable of application in clinic. The FDA-approved magnetic nanomaterial must be tested and verified. For another, the magnetothermal regulation should be more flexible.

Disk-like morphology has been found in multi-hierarchical dimensions from galaxy to red blood cell, meaning the formation of this morphology is closely relative with interaction between multiple fundamental forces during the evolution of nature. Thus, the controllable fabrication of composite materials with the disk-like micro-morphology will be favorable to both the understanding of self-assembly systems and the development of novel biomimic functional materials [26]. Moreover, the disk-like microstructure can be regarded as a contractible two-dimensional film in microscale so that some conclusions from two-dimensional film can be generalized to microdisk. Because the disk-like morphology possessed controllability in two dimensions, we thought the magnetic hydrogel with disk-like microstructure will be more flexible for electromagnetically controlled drug release. Although several engineered approaches were developed to fabricate heterogeneous composites of magnetic nanoparticles [27–29], the three-dimensionally ordered arrays of nanoparticles within soft matters such as hydrogel, have remained a challenging task.

Here, the rotation magnetic field was utilized to direct the disk-like assembly of iron oxide nanoparticles inside the PAM (polyacrylamide) hydrogel. The iron oxide nanoparticles were capped by polyglucose sorbitol carboxymethyether (PSC) and the synthesis was identically following the process flow of Ferumoxytol which was an inorganic nanodrug approved by FDA for clinical use [30]. This can guarantee the promising potential in clinical applications of our magnetic hydrogel. During the process, the reaction system was subjected to an alternating magnetic field so that the nanoparticles can form small clusters to optimize the uniformity of colloidal size and facilitate the assembly but without alteration of the composition recipe as a clinic drug [31]. The as-synthesized nanoparticles were dispersed into the monomer solution of acrylamide and a rotating magnetic field was present during whole gelation process. The rotation magnetic field can impose torques besides the dipolar forces on the magnetic nanoparticles, resulting in the rotational motion of the aligned assemblies so that it was expected to yield the disk-like assemblies. The magnetic hydrogel with different sized microstructures exhibited a dependence of magnetothermal anisotropy on size which confirmed that the magnetothermal anisotropy can exist even for the assemblies of nanoparticles in several microns.

EXPERIMENTAL SECTION

Synthesis of magnetic nanoparticles

The iron oxide nanoparticles were synthesized by co-precipitation method. Firstly, 25% (*w*/*w*) $N(CH_3)_4OH$ was slowly added into a mixture of $FeCl_2{\cdot}4H_2O$ and $FeCl_3{\cdot}6H_2O$ (molar ratio was 1:2) which was dissolved in 2.5 mL ultrapure water until pH value reached 13. Then 1.5 mL ammonium hydroxide was added into the mixture. The solution was heated to 70°C for half an hour with 600 rpm stirring during this process. Secondly, 400 mg PSC was dissolved in 3 mL ultra-pure water and added into the reaction flask. After heating for 0.5 h, the colloidal suspension was magnetically separated and washed with ultra-pure water for several times. The whole synthesis process was under the nitrogen atmosphere.

Fabrication of magnetic nanoparticles inside hydrogel

Firstly, acrylamide, ammonium persulfate and methylene-bis-acrylamide (molar ratio was 90:3:2) were added into 10 mL ultrapure water with ice bath and mixed by stirring for 5 min. Then 800 μL polymer solution and 200 μL Fe_3O_4@PSC colloidal suspension were mixed in a cylindrical glass utensil (Diameter: 1 cm, Height: 1.5 cm). After that, the mixture was subjected to a rotation magnetic field. The gelation was triggered by addition of 1 μL *N*,*N*,*N*′,*N*′-tetraethylethylenediamine. The whole process lasted for 15 min in the presence of the rotation magnetic field until the hydrogel formed.

Magnetothermal measurement

The magnetic hydrogel were subjected to an alternating magnetic field for measurement of angle-dependent magnetothermogenesis. The measurement process in the experiments continued for 20 min and the temperature was recorded by both optical fiber sensor and infrared thermo-camera.

Characterizations

The hydrodynamic size was measured by using Nano-Sizer (Zeta-Sizer, Malvern Instrument, British). The morphological characterization was done by Optical Imaging System (IX71, Olympus Co. Ltd., Japan), transmission electron microscopy (TEM, JEM-2100, Japan) and field emission scanning electron microscopy (FES-EM, Zeiss Supra 40 Gemini, Germany), micro computed tomography (micro-CT, Hiscan-M1000, China) and laser scanning confocal microscopy (Leica TCS SP8, Germany). The thermogenesis of magnetic hydrogel was measured by Fiber Spectrometer (FISO UMI 8, Canada) and Thermal Imager (Fluke, TI32). The magnetization of the samples was measured by using VSM (model 7407, Lake Shore Cryotronics, Inc., USA). The elastic compression modulus of the hydrogel was measured by a single column testing machine (Instron 5943 ITW, USA).

RESULTS AND DISCUSSION

Morphological images of the synthesized Fe_3O_4 capped by PSC nanoparticles with scanning electron microscopy (SEM) are shown in Fig. 1a. It is seen that the small nanoparticles aggregated into clusters. Hereafter, the material was denoted as Fe_3O_4@PSC nanoparticles. Average statistical diameter of the individual nanoparticles is about 13 nm based on TEM (Fig. 1b) and HR-TEM characterization (Supplementary information, Fig. S1a, b). Dynamic light scattering (DLS) measurement shows that the hydrodynamic size of the Fe_3O_4@PSC colloidal clusters is about 210 nm (Fig. S1c). Also, the Fe_3O_4@PSC colloidal clusters were negatively charged with ζ potential about −34 mV (Fig. S1d). The colloidal ζ potential of polymer monomers was also measured with approximately neural surface (−2.1 mV, Fig. S1e). Thus, the polymer monomers scarcely influence the stability of nanoparticles.

The rotating magnetic field was composed of two magnets fixed on a motor, as conceptually shown in Fig. 1c. It was found that the distance between the two magnets can significantly influence the field. Simulated field intensity in central position of the gap with different distance between the two magnets is shown in Fig. 1d, from which it can be seen that the field intensity decreases with increase of the distance. Furthermore, the uniformity of field intensity was more relative with the distance between two magnets. The field distribution between two magnets was simulated with different distance. The simulated values in the central axis were plotted in Fig. 1e, where the field intensity can be regarded uniform when the distance was above 5 cm. Otherwise, the field intensity approached the maximal value from the central position to the pole of magnets. In our experiments, the distance was set as 7 cm.

A typical sample was fabricated in the presence of a rotation magnetic field with 10 mT field intensity and 600 rpm frequency. The disk-like morphology can be recognized by optical observation from longitudinal and transverse directions, respectively (Fig. 2a, b). Here, the original images can be processed into binary images by computer to facilitate the measurement and statistics, which were also shown here. Based on the binary images, the average statistical size of diameter and thickness for the disks was about 15 μm and 5 μm, respectively. A single disk was also selectively characterized by SEM and laser scanning confocal microscopy (LSCM) more clearly, as shown in Fig. 2c and d, respectively. The local magnification indicated that the disk was composed of aggregates of nanoparticles. This can be also confirmed by the element mapping (Fig. 2e). The distribution of Fe signals exhibits the disk-like assemblies and the unconsolidated contact. The unconsolidated contact rooted in the nanoparticles themselves. Because of the standards as clinic nanodrug, the iron oxide nanoparticles were capped with a thick layer of polyglucose molecules to keep the safety and stability. Thus, the steric repulsion prevented the nanoparticles from closely-packed aggregation. Actually, the thick surface capping was the critical factor for our nanoparticles differing from the magnetic nanospheres in field-directed assembly. The hydrogel containing assemblies of nanoparticles was also observed by micro-CT. The big vision range indicated the disks were relatively uniformly dispersed inside the hydrogel (Fig. S2). However, the resolution of CT seemed too low to characterize the morphology.

The size of disk-like microstructure can be controlled by alteration of field and colloidal parameters. With field intensity increasing from 5 to 20 mT (here the colloidal concentration was 1.5 mg mL^{-1} and the frequency was 600 rpm), the morphological images of varied assemblies are shown in Fig. S3. The average statistical diameter is shown in Fig. 3a, remarkably increasing from 3 to 25 μm. Interestingly, the thickness just showed an insignificant increase, which resulted from the enhanced dipolar interaction between nanoparticles with the field intensity increasing. However, in the height direction, the magnetostatic field led to the repulsive force between particles due to the parallel arrangement of magnetic moments so that the thickness owned an insignificant increase. However, too high field was unsuitable, and it will cause the cluster-like aggregation by reason of influence from

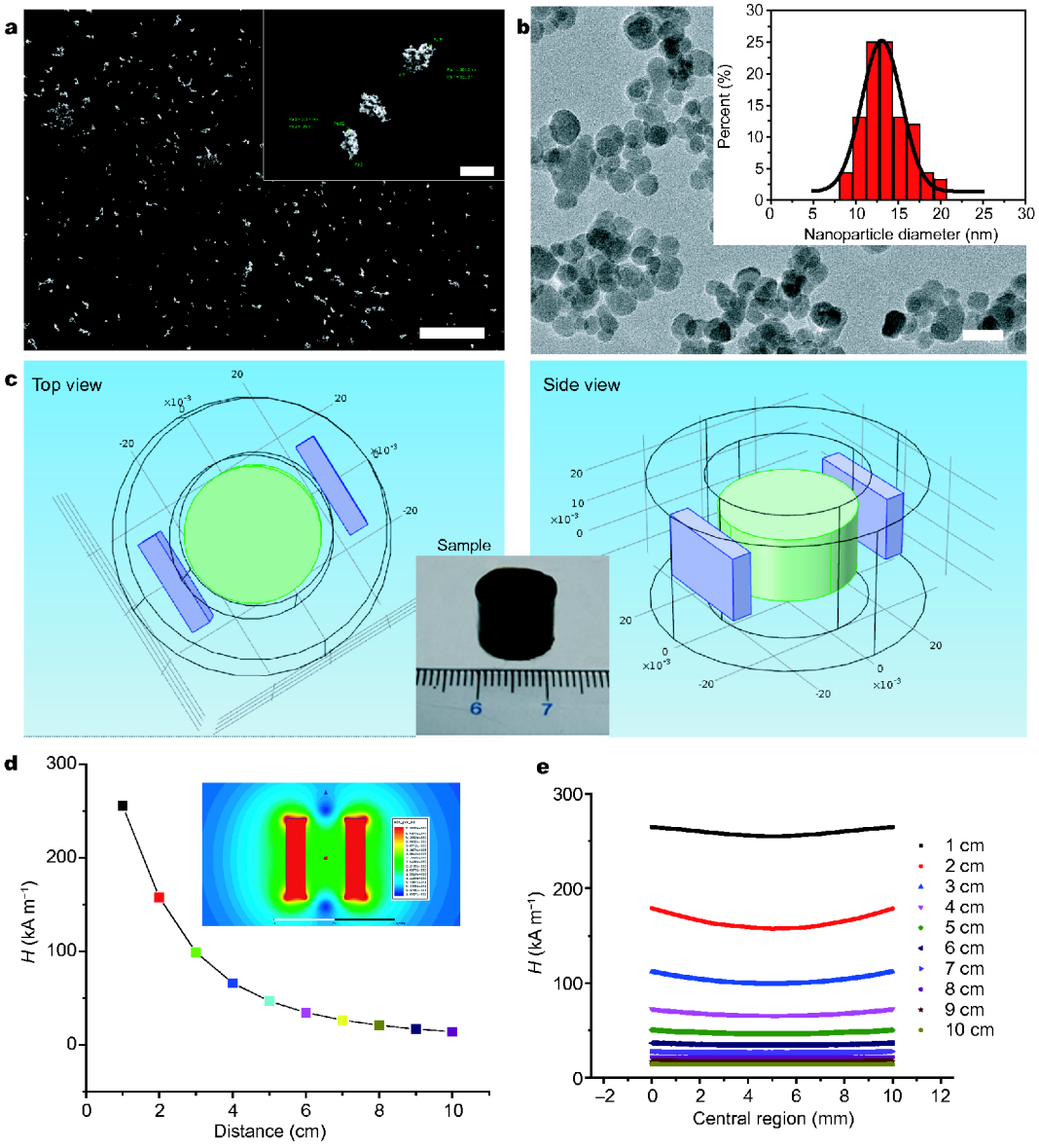

Figure 1 (a) SEM characterization of the Fe_3O_4@PSC nanoparticles (bar: 2 μm). Inset: SEM image in a larger magnification (bar: 400 nm). (b) TEM characterization of the Fe_3O_4@PSC nanoparticles, and the average statistics diameter is shown in the insert figure (bar: 20 nm). (c) Top and side views of a conceptual rotating magnetic field platform, and the magnet hydrogels sample. (d) Simulated magnetic field intensity of center point with distance between two magnets (inset: magnetic field simulation). (e) The simulated magnetic field intensity in central region by adjusting the distance between two poles from 1 to 10 cm.

the field gradient. When the field intensity was over 30 mT, the magnetic nanoparticles were experimentally found to move toward edge of the hydrogels (Fig. S4). On the contrary, the increase of field frequency seemed to prohibit the expansion of microdisks. In case that the field intensity (10 mT) and the colloidal concentration (1.5 mg mL^{-1}) were fixed, the morphological images of microdisks under different field frequency were shown in Fig. S5. The average statistical diameter of assembled disks decreased from 22 μm at 100 rpm to 13 μm at 1,200 rpm (Fig. 3b). Meanwhile, the average statistical thickness increased from 3 to 8 μm. Here centrifugal force can account for this result. It was thought that the exterior nanoparticles will be cast off by the centrifugal force with the increase of rotational speed. However, the possibility of antiparallel magnetic moments between two assemblies was augmented in the height direction so that the thickness increased. During our experiments, the colloi-

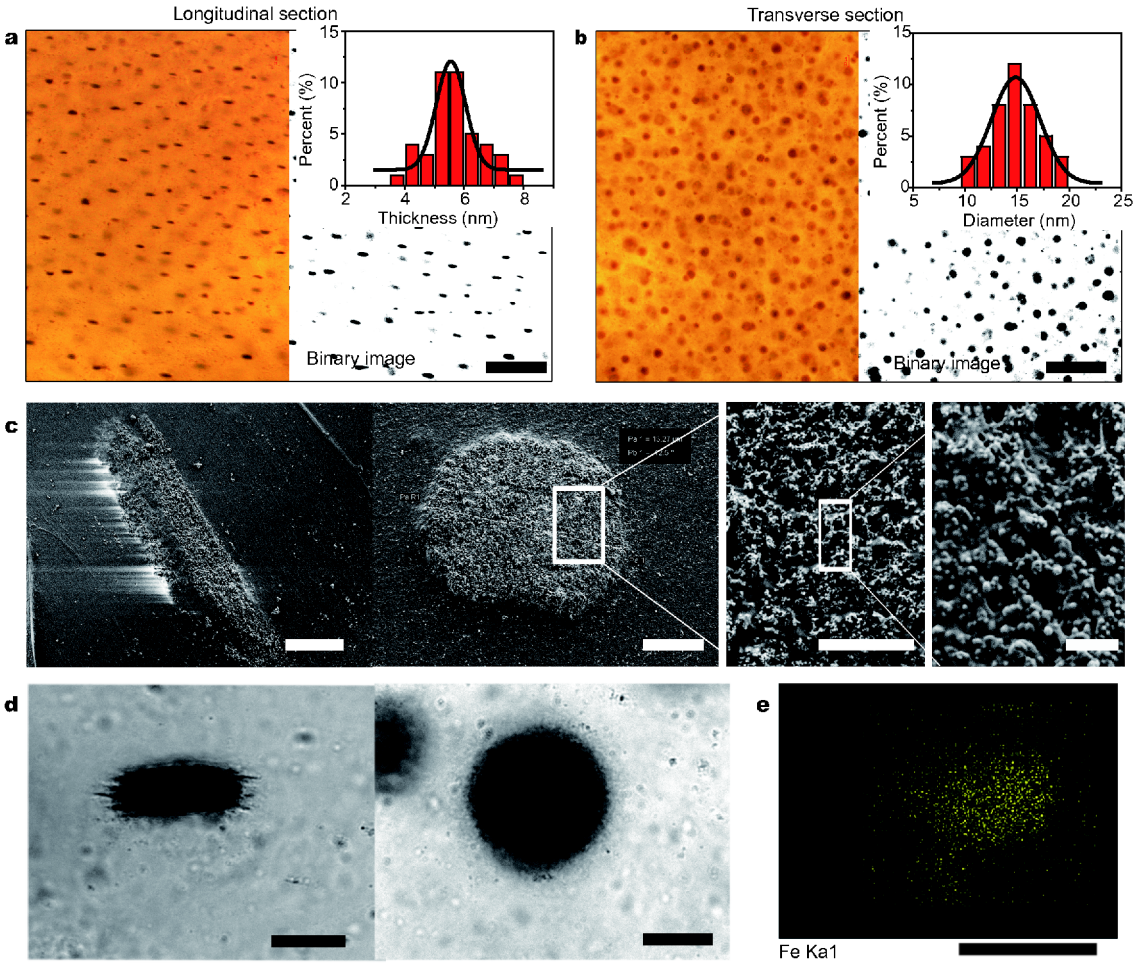

Figure 2 Characterization of a typical magnetic hydrogel sample. (a) The longitudinal section of magnetic hydrogel in optical imaging (bar: 100 μm). Right part of the figure was the corresponding binary image. (b) The transverse section of magnetic hydrogel in optical imaging (bar: 100 μm). (c) The longitudinal (bar: 4 μm) and transverse (bar: 4 μm) SEM images of a single microdisk and the local magnification (bar: 2 μm and 200 nm). (d) The longitudinal section (bar: 10 μm) and transverse section (bar: 10 μm) LSCM images of a single microdisk. (e) Fe element mapping of a single microdisk (bar: 10 μm).

dal concentration was found to play a critical role in the formation of disk-like microstructure. The average statistical diameter and thickness of samples with different concentration were shown in Fig. 3c and the morphological images were shown in Fig. S6. Here the field intensity and frequency were fixed at 10 mT and 600 rpm, respectively. The average statistical diameter of assembled disks increased from 2 to 17 μm with the increase of colloidal concentration. It was worth noting that the thickness here showed an insignificant alteration. This phenomenon can be interpreted by the reduced distance between nanoparticles which reinforced the dipolar interaction in the planar direction but insignificantly influence the repulsive force between magnetic particles in the height direction. However, too high concentration was also unsuitable. The colloidal nanoparticles were unable to form the disk-like assemblies under concentration of 2.3 mg mL^{-1}. Instead, the twisted chain-like assemblies can be obviously observed (Fig. S7). Here fluid resistance can account for this result. If the size of chain-like assemblies were too big, the fluidic drag force will also be reinforced according to the Stokes Law. This force will hinder the twisting process of colloidal assemblies so that the disk-like structure could not be formed under too high concentration. It should be mentioned that the influence of different factors were coupled rather than isolated. By synergistically adjustment of the field and colloidal parameters, the size of microstructures can be controlled from less than 7 μm to about 23 μm (Fig. 3d).

This result demonstrated that the formation of disk-like

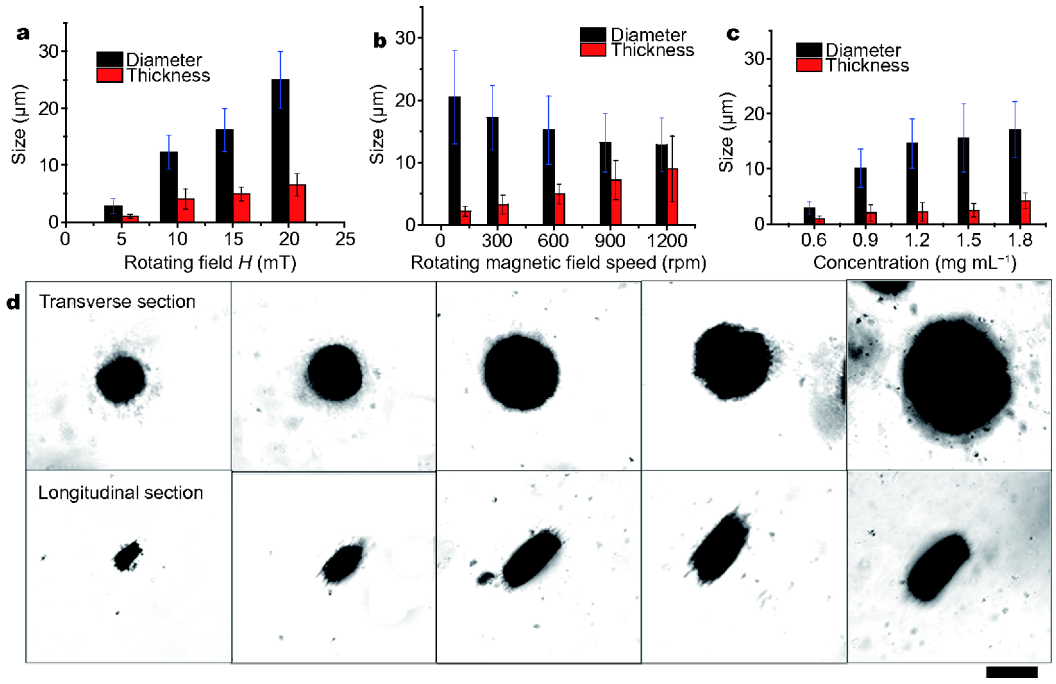

Figure 3 (a) Average statistical size of the microstructure with alteration of field intensity. (b) Average statistical size of the microstructure with alteration of field frequency. (c) Average statistical size of the microstructure with alteration of colloidal concentration. (d) LSCM characterization of a series of microdisks with different size (Diameter from the left to the right: 7, 12, 15, 18 and 23 μm. Thickness from the left to the right: 3, 5, 7, 8 and 8 μm. Bar: 10 μm).

assemblies should result from the rotational aggregation of colloidal clusters. The clusters were initially formed under the directional action of magnetic field so that the clusters showed somewhat chain-like morphology. However, due to the rotation of the magnetic field, the chain-like clusters could not grow continuously. The chain-like clusters then twisted together to form the disk-like structures in the presence of torsional force resulting from the rotation magnetic field. The morphology of nanoparticles inside the hydrogel in different stages during the assembly can be characterized by SEM after freeze dehydration of sliced hydrogel sample. Here, five morphological images were sampled to show the formation process. Initially, the magnetic nanoparticles were randomly dispersed inside the hydrogel (Fig. 4a). Just after the rotation magnetic field was applied, it can be seen that the magnetic particles began to aggregate showing the tendency of one-dimensional assembly (Fig. 4b). Then, the assemblies of nanoparticles continued to grow in the presence of the rotation magnetic field and the nanoparticles can be seen to gradually aggregate together around a core (Fig. 4c, d). Finally, the disk-like assemblies of magnetic nanoparticles formed where the nanoparticles aggregated together more closely (Fig. 4e). Therefore, the formation mechanism can be demonstrated based on the coupled interaction of magnetic dipolar force (F_{mag}), torsional force (F_{tor}) from the rotation field and viscous resistance from fluid (F_{drag}), which was schematically illustrated in Fig. 4f. As far as the formation of disk-like morphology was concerned, it was actually due to the principle of energy minimization. It is known that demagnetization energy plays a dominant role in the assembly of magnetic nanomaterials [32–35]. The energy fluctuation for different morphology of assemblies in the presence of rotation magnetic field was simulated by Object Oriented Micromagnetic Framework (OOMMF), confirming that the disk-like structure was the minimal state of magnetic energy (Fig. 4g). Thus, in the presence of rotating magnetic field, the nanoparticles will evolve into the densely packed state eventually, which was directed by the external field from a discrete system into an equilibrium state.

For the one- or two-dimensional assemblies of magnetic nanoparticles in centimeter scale, we have proved that the assembly can enhance the couplings between nanoparticles so that the assemblies will show some properties resembling the bulk materials, leading to emergence of the orientation-dependent magnetothermogenesis. Here, the disk-like microstructure magnetic hydrogel similarly exhibited the orientation-

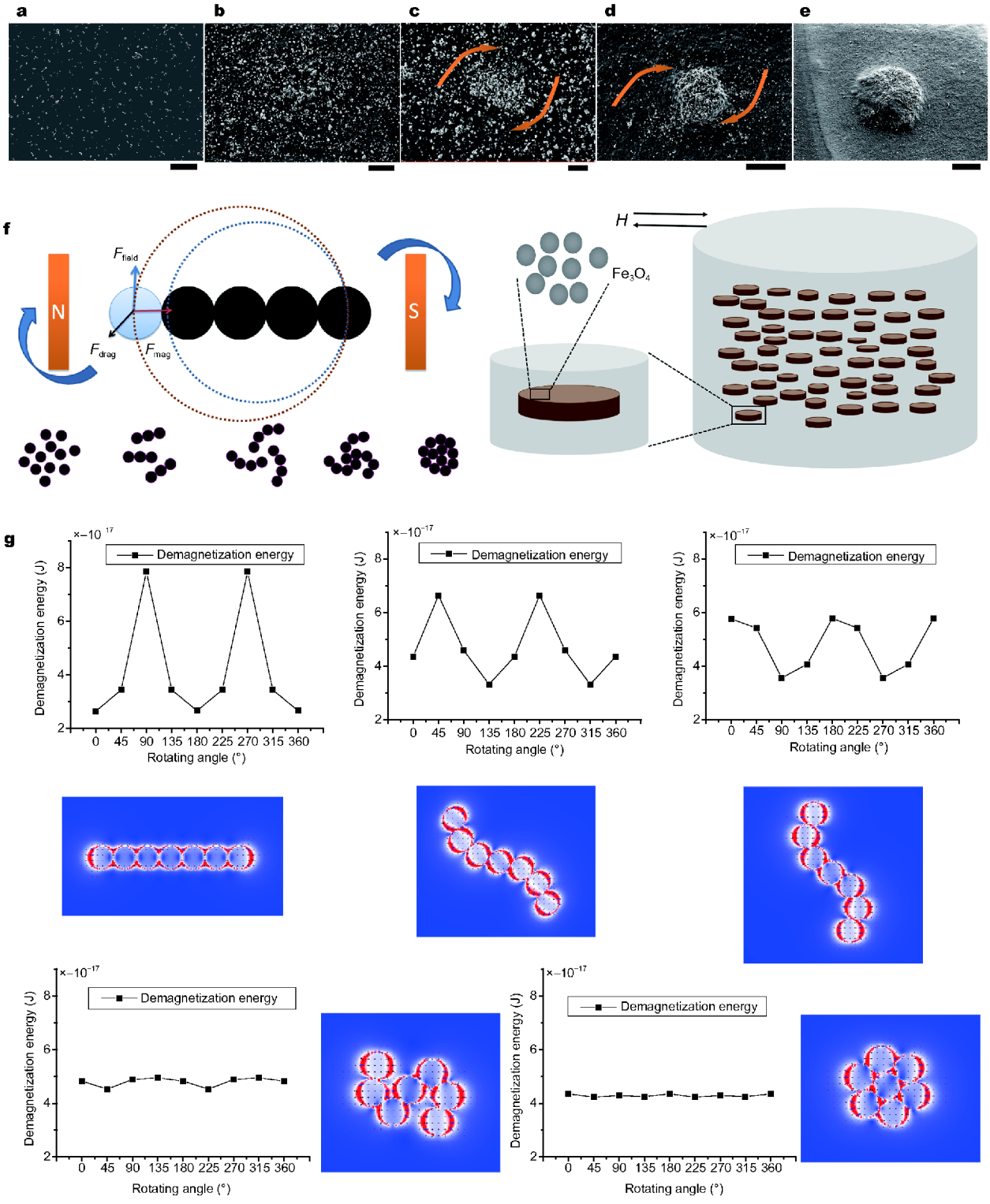

Figure 4 A possible mechanism for the formation of disk-like structure. (a) The iron oxide nanoparticles inside hydrogel at initial state (bar: 2 μm). (b) At the beginning of rotating magnetic field (bar: 2 μm). (c) With continuing rotating magnetic field (bar: 1 μm). (d) Intermediate state (bar: 2 μm). (e) Final state (bar: 4 μm). (f) Schematic diagram of formation process based on three forces. (g) OOMMF simulations of the demagnetization energy variation in angle range from 0° to 360° for different assembled morphology in the presence of a rotating magnetic field.

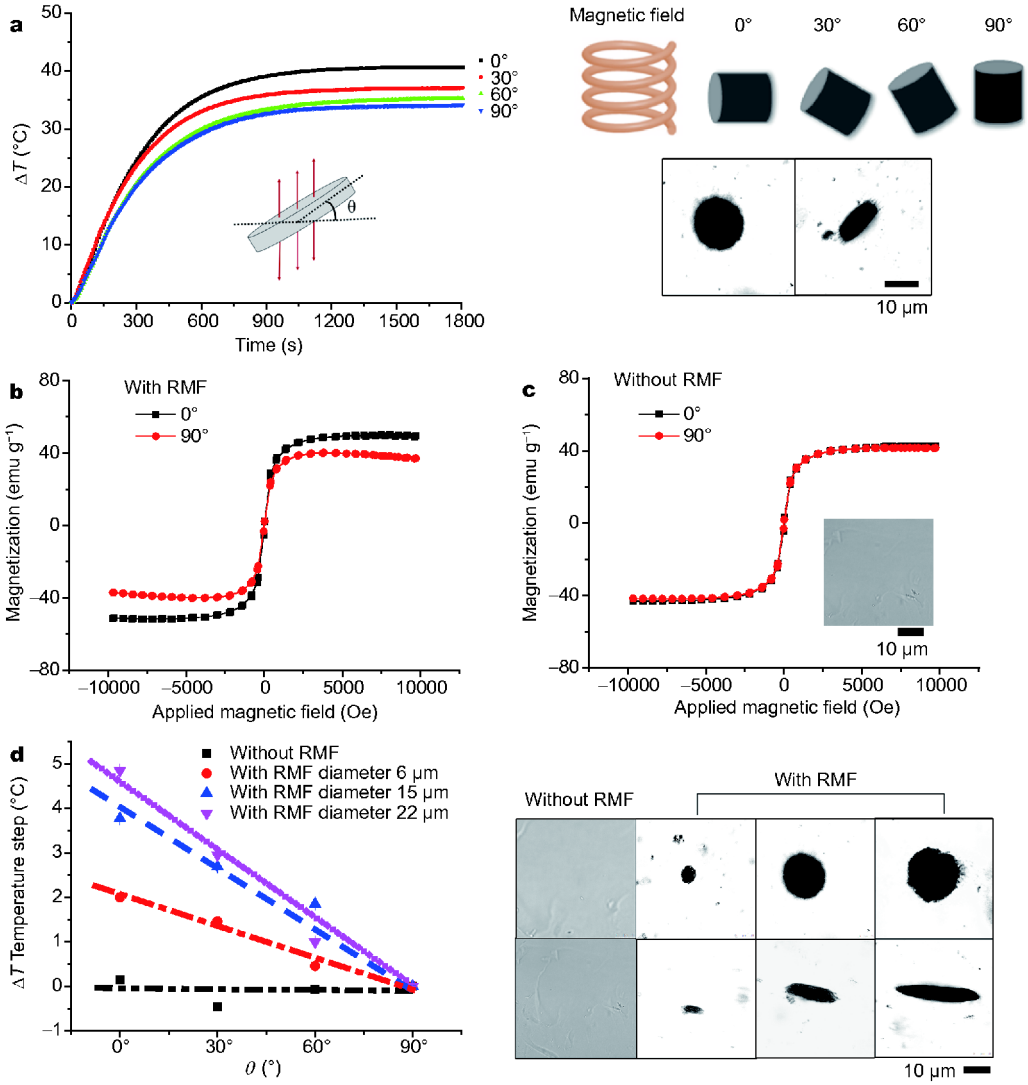

Figure 5 (a) Magnetothermal measurements of an assembled magnetic hydrogel with the different incident direction of alternating magnetic field (0°, 30°, 60° and 90°). (b and c) The hysteresis loops for assembled magnetic hydrogel and disorganized magnetic hydrogel, respectively. (d) Comparison of anisotropy degree for the assembled magnetic hydrogels with different size and the disorganized magnetic hydrogel. Average statistical diameters for the three assembled magnetic hydrogel were 6, 15 and 22 μm, respectively. Average statistical thicknesses were 3, 4 and 4 μm, respectively.

dependent magnetothermogenesis even in micron scale. Temperature curves of the magnetic hydrogel in different slope angles confirmed this point, which were shown in Fig. 5a. The corresponding 2D mapping images by infrared thermo-camera were shown in Fig. S8. VSM measurements of the assembled and the disorganized magnetic hydrogels exhibited that the magnetic microstructures owned obvious anisotropy of magnetization after assembly (Fig. 5b, c). This result demonstrated the magnetothermal anisotropy resulted from the anisotropic morphology after assembly. Interestingly, the anisotropy degree of the assembled microdisks was augmented with the increase of microdisk size. The magnetothermogenic data for three microdisks of different size and the disorganized sample were shown in Fig. S9. From these data, we compared the thermogenic increment between different samples with alteration of the incident direction of alternating magnetic field. The results were shown in Fig. 5d. By data fitting, it can be seen clearly that the slope of thermogenic increment to field direction was getting bigger with the increase of microdisk size. The higher slope meant the variance of thermogenesis was more significant for the sample under the alternating magnetic field with different incident directions. Here the ther-

mogenesis was identical in the different incident direction of field for the disorganized sample, meaning its thermogenesis was isotropic in the presence of alternating magnetic field with different incident directions. This result was important because it proved the assembly-induced anisotropy for collective magnetic nanoparticles still remained true even for the assemblies of several microns. Moreover, the anisotropy degree of magnetic hydrogel can also be tuned by alteration of microstructure size, which provided us a more flexible route to control the thermogenesis as well as the drug release of magnetic hydrogel by alternating magnetic field.

In addition, the hydrogel's mechanical property was also influenced by the microstructure of nanoparticles. Here, the compressive moduli were measured for the plain hydrogel, the magnetic hydrogel with disordered nanoparticles and the magnetic hydrogel with disk-like assemblies (Fig. S10). Based on the results, the elastic modulus was significantly reinforced by addition of iron oxide nanoparticles into the hydrogel. This is obviously because of the increased portion of 'hard spheres'. Furthermore, the formation of ordered microstructure can promote the compressive modulus. More interestingly, the compressive modulus parallel to the assembled disks was significantly larger than that perpendicular to the assembled disks. This result manifested that the assembled microstructure of iron oxide nanoparticles can also influence the mechanical property of composite hydrogel.

CONCLUSIONS

In summary, one facile route was developed to fabricate the composite hydrogel with disk-like microstructure of iron oxide nanoparticles whose size can be regulated at least from 7 to 23 μm. The assembled magnetic hydrogel exhibited the controllable anisotropy degree dependent upon the size of microstructure. This work demonstrated that the field-directed assembly will be a promising route for automatic, intelligent and rapid fabrication of composite materials with controllable internal microstructures that will provide an effective means to control the property of composite materials containing functional nanoparticles. The iron oxide nanomaterial in this work is FDA-approved so that the magnetic hydrogel with ordered microstructure is highly promising for future clinical translation.

Received 10 December 2017; accepted 27 January 2018; published online 6 March 2018

1 Park SB, Lih E, Park KS, *et al.* Biopolymer-based functional composites for medical applications. Prog Polymer Sci, 2017, 68: 77–105
2 Lin N, Cao L, Huang Q, *et al.* Functionalization of silk fibroin materials at mesoscale. Adv Funct Mater, 2016, 26: 8885–8902
3 Chang H, Luo J, Gulgunje PV, *et al.* Structural and functional fibers. Annu Rev Mater Res, 2017, 47: 331–359
4 Kim CR, Uemura T, Kitagawa S. Inorganic nanoparticles in porous coordination polymers. Chem Soc Rev, 2016, 45: 3828–3845
5 Cezar CA, Mooney DJ. Biomaterial-based delivery for skeletal muscle repair. Adv Drug Deliver Rev, 2015, 84: 188–197
6 Arslan E, Garip IC, Gulseren G, *et al.* Bioactive supramolecular peptide nanofibers for regenerative medicine. Adv Healthcare Mater, 2014, 3: 1357–1376
7 Mendes AC, Baran ET, Reis RL, *et al.* Self-assembly in nature: using the principles of nature to create complex nanobiomaterials. WIREs Nanomed Nanobiotechnol, 2013, 5: 582–612
8 Mouw JK, Ou G, Weaver VM. Extracellular matrix assembly: a multiscale deconstruction. Nat Rev Mol Cell Biol, 2014, 15: 771–785
9 Rising A, Johansson J. Toward spinning artificial spider silk. Nat Chem Biol, 2015, 11: 309–315
10 Wong Po Foo C, Patwardhan SV, Belton DJ, *et al.* Novel nanocomposites from spider silk-silica fusion (chimeric) proteins. Proc Natl Acad Sci USA, 2006, 103: 9428–9433
11 Yin X, Mead BE, Safaee H, *et al.* Engineering stem cell organoids. Cell Stem Cell, 2016, 18: 25–38
12 Quarta M, Brett JO, DiMarco R, *et al.* An artificial niche preserves the quiescence of muscle stem cells and enhances their therapeutic efficacy. Nat Biotechnol, 2016, 34: 752–759
13 Le Ferrand H, Bouville F, Niebel TP, *et al.* Magnetically assisted slip casting of bioinspired heterogeneous composites. Nat Mater, 2015, 14: 1172–1179
14 Wang M, He L, Yin Y. Magnetic field guided colloidal assembly. Mater Today, 2013, 16: 110–116
15 Xu X, Li H, Zhang Q, *et al.* Self-sensing, ultralight, and conductive 3D graphene/iron oxide aerogel elastomer deformable in a magnetic field. ACS Nano, 2015, 9: 3969–3977
16 Ahniyaz A, Sakamoto Y, Bergström L. Magnetic field-induced assembly of oriented superlattices from maghemite nanocubes. Proc Natl Acad Sci USA, 2007, 104: 17570–17574
17 Martin JE, Snezhko A. Driving self-assembly and emergent dynamics in colloidal suspensions by time-dependent magnetic fields. Rep Prog Phys, 2013, 76: 126601
18 Snezhko A, Aranson IS, Kwok WK. Surface wave assisted self-assembly of multidomain magnetic structures. Phys Rev Lett, 2006, 96: 078701
19 Thévenot J, Oliveira H, Sandre O, *et al.* Magnetic responsive polymer composite materials. Chem Soc Rev, 2013, 42: 7099–7116
20 Kango S, Kalia S, Celli A, *et al.* Surface modification of inorganic nanoparticles for development of organic–inorganic nanocomposites—A review. Prog Polymer Sci, 2013, 38: 1232–1261
21 Thoniyot P, Tan MJ, Karim AA, *et al.* Nanoparticle-hydrogel composites: concept, design, and applications of these promising, multi-functional materials. Adv Sci, 2015, 2: 1400010
22 Hu K, Sun J, Guo Z, *et al.* A novel magnetic hydrogel with aligned magnetic colloidal assemblies showing controllable enhancement of magnetothermal effect in the presence of alternating magnetic field. Adv Mater, 2015, 27: 2507–2514
23 Nair M, Guduru R, Liang P, *et al.* Externally controlled on-demand release of anti-HIV drug using magneto-electric nanoparticles as

carriers. Nat Commun, 2013, 4: 1707
24 Sun J, Fan F, Wang P, *et al.* Orientation-dependent thermogenesis of assembled magnetic nanoparticles in the presence of an alternating magnetic field. ChemPhysChem, 2016, 17: 3377–3384
25 Fan F, Liu J, Sun J, *et al.* Magnetic energy-based understanding the mechanism of magnetothermal anisotropy for macroscopically continuous film of assembled Fe_3O_4 nanoparticles. AIP Adv, 2017, 7: 085109
26 Qian Y, Zhang X, Qi D, *et al.* Thin-film organic semiconductor devices: from flexibility to ultraflexibility. Sci China Mater, 2016, 59: 589–608
27 Martin JJ, Fiore BE, Erb RM. Designing bioinspired composite reinforcement architectures via 3D magnetic printing. Nat Commun, 2015, 6: 8641
28 Richardson JJ, Björnmalm M, Caruso F. Technology-driven layer-by-layer assembly of nanofilms. Science, 2015, 348: aaa2491–aaa2491
29 Wang J, Cheng Q, Lin L, *et al.* Synergistic toughening of bioinspired poly(vinyl alcohol)–clay–nanofibrillar cellulose artificial nacre. ACS Nano, 2014, 8: 2739–2745
30 Chen B, Li Y, Zhang X, *et al.* An efficient synthesis of ferumoxytol induced by alternating-current magnetic field. Mater Lett, 2016, 170: 93–96
31 Li Y, Hu K, Chen B, *et al.* Fe_3O_4@PSC nanoparticle clusters with enhanced magnetic properties prepared by alternating-current magnetic field assisted co-precipitation. Colloids Surfs A-Physicochem Eng Aspects, 2017, 520: 348–354
32 Aharoni A. Demagnetizing factors for rectangular ferromagnetic prisms. J Appl Phys, 1998, 83: 3432–3434
33 Bergmann G, Lu JG, Tao Y, *et al.* Frustrated magnetization in Co nanowires: Competition between crystal anisotropy and demagnetization energy. Phys Rev B, 2008, 77: 054415
34 Normile PS, Andersson MS, Mathieu R, *et al.* Demagnetization effects in dense nanoparticle assemblies. Appl Phys Lett, 2016, 109: 152404
35 Yuan J, Gao H, Schacher F, *et al.* Alignment of tellurium nanorods *via* a magnetization–alignment–demagnetization ("MAD") process assisted by an external magnetic field. ACS Nano, 2009, 3: 1441–1450

Acknowledgements This work was supported by the National Key Research and Development Program of China (2017YFA0104301). Sun J is thankful to the Fundamental Research Funds for the Central Universities. Fan F, Sun J, Ma M and Gu N appreciate the supports from Collaborative Innovation Center of Suzhou NanoScience and Technology.

Author contributions Fan F and Sun J designed and operated the experiments; Chen B and Li Y provided the iron oxide sample. Hu K and Wang P gave some useful advice for our experiments; Ma M contributed to the theoretical analysis. Gu N provided experimental ideas, guided the experimental process. All authors contributed to the general discussion.

Conflict of interest The authors declare that they have no conflict of interest.

Supplementary information Supporting materials are available in the online version of the paper.

Fengguo Fan is pursuing his PhD degree in biomedical engineering at Southeast University. His research interest is the assembly of nanoparticles.

Jianfei Sun received his PhD degree in biomedical engineering from Southeast University in 2008. He is now an associate professor at the School of Biological Science and Medical Engineering, Southeast University. His research interests include the fabrication of nanoelectronic devices by self-assembly of nanoparticles and their application in biomedical issues.

Ning Gu received his PhD degree in biomedical engineering from the Department of Biomedical Engineering, Southeast University, Nanjing, China, in 1996. Currently he is a Cheung Kong Scholar Chair Professor at the School of Biological Science and Medical Engineering, Southeast University.

旋转磁场调控组装圆盘状微结构磁性水凝胶

范凤国[1,2], 孙剑飞[1*], 陈博[1], 李杨[1], 胡克[3], 王鹏[4], 马明[1], 顾宁[1*]

摘要 具有可控微结构的复合生物材料在组织工程和再生医学中发挥着越来越重要的作用. 本文报道了在旋转磁场作用下, 通过组装氧化铁纳米颗粒制备具有盘状微结构的磁性水凝胶复合材料. 组装用的磁性纳米材料是按照合成Ferumoxytol的方法制备而得, 也是唯一的被FDA批准应用于临床的铁氧化物纳米颗粒. 磁性纳米颗粒的微观结构在水凝胶内部排列为三维有序. 其形成机理是由于磁性纳米颗粒的排列链受到旋转磁场作用扭曲从而形成了微观结构系统能量的最低态. 通过改变组装参数, 可以将微结构尺寸从几微米调整到几十微米. 随着组装结构体的增大, 其磁各向异性也得到相应的增强. 这种情况也证明了即使是微米级的纳米粒子聚集体, 也可以通过旋转磁场组装诱导产生各向异性. 旋转磁场辅助技术制备有序微纳米结构水凝胶具有成本低、操作简单、灵活等优点. 我们相信利用这种方法将有利于构建一些快速、绿色和智能制造的复合材料.

